Duan *et al. Animal Diseases* (2023) 3:38
https://doi.org/10.1186/s44149-023-00100-z

Animal Diseases

ORIGINAL ARTICLE

Open Access

The generation of hemagglutinin monoclonal antibodies against H9N2 influenza virus

Yongcheng Duan[1], Qingli Guo[1], Shaoyu Tu[1], Jiahui Zou[1], Guohong Li[2], Cheng Liang[2], Yanqing Cheng[1], Yijie Zhou[1], Lin Chen[1], Yuanbao Zhou[1], Sizhu Suolang[3*] and Hongbo Zhou[1,3,4,5*]

Abstract

H9N2 avian influenza viruses (AIVs) are widely distributed, causing continuous outbreaks in poultry and sporadic infections in humans. Vaccination is the primary method used to prevent and control H9N2 AIV infection. However, the ongoing evolution and mutation of AIVs often result in limited protection effects from vaccines. Therapeutic monoclonal antibodies (mAbs) targeting influenza viruses offer a promising alternative. In this study, we immunized mice with inactivated H9N2-W1 virus, and we screened and acquired five mAbs, namely 4D12, F4, 5C8, 2G8 and A11. We showed that all five mAbs specifically targeted the HA protein of various H9N2 AIV strains. In vitro neutralization tests demonstrated that all five mAbs exhibited neutralization activity against H9N2 AIVs, with mAb F4 displaying the most potent neutralization effect. The F4 mAb exhibited dose-dependent preventive and therapeutic effects against lethal H9N2-115 infection, and the administration of F4 at a dose of 3 μg/g provided complete protection in vivo. Our study presents an alternative approach for preventing and controlling H9N2 AIV infection. Furthermore, the identified F4 mAb holds promise as a solution to potential pandemics in humans caused by H9N2 AIVs.

Keywords AIV, mAb, Neutralization, Preventive, Therapeutic

Introduction

H9N2 avian influenza viruses (AIVs) were initially isolated in the United States in 1966 and have since been reported in various countries (Carnaccini and Perez 2020; Mortimer 2019). Initially, H9N2 AIVs were found exclusively in ducks in Asia without causing any severe symptoms (Alexander 2007). However, during the late 20th century, H9N2 AIVs gradually spread to chickens in several Asian countries (Pusch and Suarez 2018; Xu et al. 2007). H9N2 AIVs have the ability to induce immunosuppression in infected hosts, leading to complicated mixed infections with bacteria and other viruses (Hajam et al. 2018; Horwood et al. 2018; Li et al. 2018; Shanmuganatham et al. 2013). This complexity poses challenges for disease control and prevention, resulting in substantial economic losses for the global poultry industry. Moreover, H9N2 AIVs exhibit a broad host range,

*Correspondence:
Sizhu Suolang
xzslsz@xza.edu.cn
Hongbo Zhou
hbzhou@mail.hzau.edu.cn
[1] National Key Laboratory of Agricultural Microbiology, College of Veterinary Medicine, Huazhong Agricultural University, Wuhan, Hubei, P. R. China
[2] Wuhan Keqian Biological Co., Ltd, Wuhan, Hubei, P. R. China
[3] Department of Animal Science, Tibet Agricultural and Animal Husbandry College, Nyingchi, P. R. China
[4] Hubei Hongshan Laboratory, Wuhan, Hubei, P. R. China
[5] Frontiers Science Center for Animal Breeding and Sustainable Production, Wuhan, Hubei, P. R. China

capable of infecting not only birds but also crossing species barriers to infect mammals, including humans (Gu et al. 2017; Peacock et al. 2019). Since H9N2 AIVs were first confirmed to infect humans in 1999, interspecies transmission of this subtype of AIV has occasionally been reported worldwide (Peiris et al. 1999). To date, H9N2 AIVs have been reported to cause 112 human infection cases (Adlhoch et al. 2022; Li et al. 2022). Therefore, urgent measures are required for the prevention and control of H9N2 AIVs.

Similar to other viral diseases, there are currently no highly effective methods for preventing and treating avian influenza, and vaccination remains the most commonly used means to prevent its occurrence and spread (Subbarao and Joseph 2007). In recent years, the continuous development of molecular biology techniques has provided a theoretical foundation and technical means for the development of novel vaccines against avian influenza. In addition to traditional inactivated vaccines, exploration has been conducted in the field of genetically engineered vaccines, including live-vector vaccines, subunit vaccines, and nucleic acid vaccines (De Pinho Favaro et al. 2022; Wang et al. 2022b). However, as AIV continues to evolve and mutate, the vaccines often do not match the currently circulating strains, resulting in limited protection provided by vaccines (Dong et al. 2022).

Drugs targeting matrix proteins M2, neuraminidase, and polymerase have been approved by the FDA and applied for controlling influenza virus infections (Caceres et al. 2022). However, the effectiveness of these drugs has been hindered by the emergence of resistant strains with mutations, such as Ser31Asn, Leu26Ile and Val27Ala on M2; His274Tyr, Ile117Val, Glu119Ala and Arg292Lys on NA; and Ile38Thr, Ile38Phe and Ile38Met on the polymerase subunit PA (Abed et al. 2005; Dong et al. 2015; Imai et al. 2020; Mahal et al. 2021; Musharrafieh et al. 2019; Takashita et al. 2019). Monoclonal antibodies (mAbs) have alternatively gained increasing attention as they are characterized by their specificity and ability to enhance immune responses, making them a potential treatment and prevention option for influenza (Carter and Rajpal 2022).

Muromonab-CD3 (OKT3) was the first therapeutic monoclonal antibody approved by the FDA in 1985 for preventing rejection reactions during kidney, heart, and liver transplantation (Kuhn and Weiner 2016). Since then, an increasing number of antibody-related drugs have been applied in clinical treatment, with over 100 antibody-based treatments currently approved for severe human diseases (Kaplon et al. 2022). During the COVID-19 pandemic, monoclonal antibody therapies have also played a vital role (Corti et al. 2021a). Hemagglutinin (HA) serves as the primary surface protein of influenza viruses, and host-induced neutralizing antibodies mainly target HA. Over the past few decades, researchers have made significant efforts to identify highly conserved epitopes in HA and develop broadly neutralizing antibodies against influenza. Presently, certain mAbs are undergoing clinical trials for the treatment of influenza (Corti et al. 2016; Ekiert et al. 2009; Ekiert et al. 2011; Gerhard et al. 2006; Kallewaard et al. 2016; Lim et al. 2016; Wollacott et al. 2016).

In this study, we immunized mice with inactivated H9N2-W1 virus and identified five mAbs targeting H9N2 AIV HA. We evaluated the neutralizing activity of these antibodies at the cellular level and demonstrated their effectiveness against H9N2 AIVs. In prophylactic and therapeutic trials, the monoclonal antibody F4, administered at a dose of 3 μg/g, provided complete protection against lethal H9N2-115 infection, indicating its potential application in preventing and treating H9N2 AIV outbreaks.

Results

Generation and characterization of mAbs against H9N2 AIVs

To generate mAbs against H9N2 AIVs, we intranasally immunized 6-week-old Balb/c mice with inactivated H9N2-W1 AIV. The immunization procedure, as diagramed in Fig. 1A, involved subcutaneous multipoint injection of the inactivated vaccine followed by additional three booster vaccinations at 15-day intervals. Serum samples were collected on day 10 after the third immunization, and antibody levels were determined using indirect enzyme-linked immunosorbent assay (ELISA) and hemagglutination inhibition (HI) assays (Fig. 1B-C). The results showed that the serum ELISA titer and HI titer of mice immunized with inactivated H9N2-W1 were above 1:204, 800 and 2^9, respectively.

Subsequently, the fusion of SP2/0 myeloma cells with splenocytes from immunized mice was induced using PEG (Fig. 2A). Antibody-positive hybridoma cell lines were screened using indirect ELISA with inactivated viruses as coating antigens (Fig. 2B) and HI assays (Fig. 2C). Through limited dilution subcloning, five stable and continuously antibody-secreting cell lines were identified, namely 4D12, F4, 5C8, 2G8 and A11. To confirm the successful hybridization of the hybridoma cells, antibody-positive cells in the logarithmic growth phase were treated with colchicine to halt cell division. Microscopic analysis revealed that the number of chromosomes in SP2/0 cells was approximately 65 pairs, while the H9N2 antibody-positive hybridoma cell lines exhibited approximately 100 pairs of chromosomes (Fig. 2D), indicating successful cell fusion. The monoclonal antibodies were further characterized using the mAb-subclass

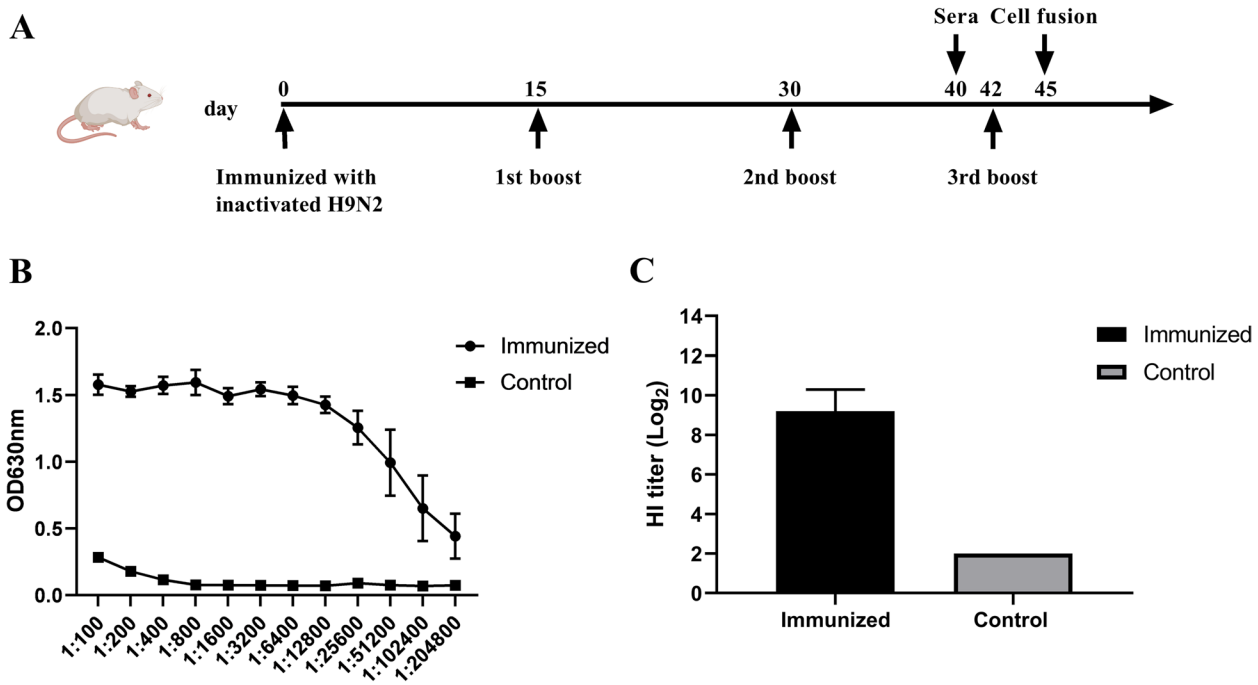

Fig. 1 Preparation and generation of monoclonal antibodies. **A** Diagram of the mouse immunization procedure. (B-C) Antibody titer assessment. Serum samples collected 10 days after the third immunization were analyzed to determine the specific antibody titer using both the **B** indirect ELISA and **C** hemagglutination inhibition (HI) assay

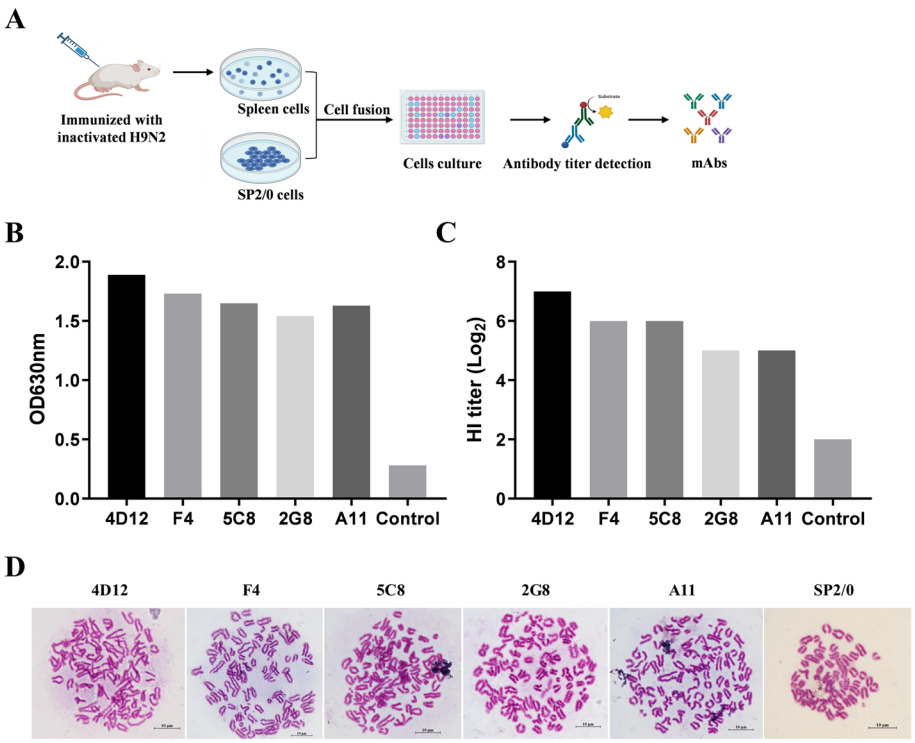

Fig. 2 Screening of mAbs positive for H9N2. **A** Diagram of the murine mAb production process. (**B-C**) Screening results of antibody-positive hybridoma cells by **B** ELISA detection and **C** hemagglutination inhibition detection of antibody titers in the supernatant of hybridoma cells. **D** Chromosome staining of antibody-positive hybridoma cell lines and SP2/0 myeloma cells. Scale bars = 10 μm

identification enzyme kit. The results showed that all monoclonal antibodies had a heavy chain subtype of IgG1 and a light chain subtype of Kappa (Table 1).

Reactivities of mAbs to multiple viral strains

To obtain large quantities of monoclonal antibodies, 8-week-old Balb/c mice pretreated with Freund's incomplete adjuvant were intraperitoneally inoculated with H9N2 antibody-positive hybridoma cell lines. The results showed that the HI titer of mouse ascites was above 2^{15} (Fig. 3A). Subsequently, the antibodies were collected and purified. SDS–PAGE and Coomassie Blue staining confirmed the presence of heavy and light chains for each monoclonal antibody (Fig. 3B). Western blot results revealed targeting bands above 70 kDa (Fig. 3C), corresponding to the influenza virus HA protein. In vitro neutralization assays were performed to assess the antiviral effects of the mAbs against multiple virus strains. The results demonstrated that all screened mAbs effectively neutralized various strains of H9N2 influenza viruses, including H9N2-W1, H9N2-115 and H9N2-SH13, which all belong to the Y280-like lineage (Fig. S1). Among them, mAb F4 exhibited the most potent neutralizing effect. However, none of the screened mAbs showed reactivity with the H1 subtype strains (Table 2). The characteristics of the mAbs were additionally verified through indirect immunofluorescence assays (IFAs). Confocal microscopy demonstrated the desirable reactivity of all five monoclonal antibodies with H9N2-W1 and H9N2-115 (Fig. 3D). Taken together, the screened mAbs exhibited a neutralizing effect on H9 subtype strains.

Table 1 Isotype identification of H9N2 AIV mAbs

Cell line	Heavy chain	Light chain
4D12	IgG1	kappa
F4	IgG1	kappa
5C8	IgG1	kappa
2G8	IgG1	kappa
A11	IgG1	kappa

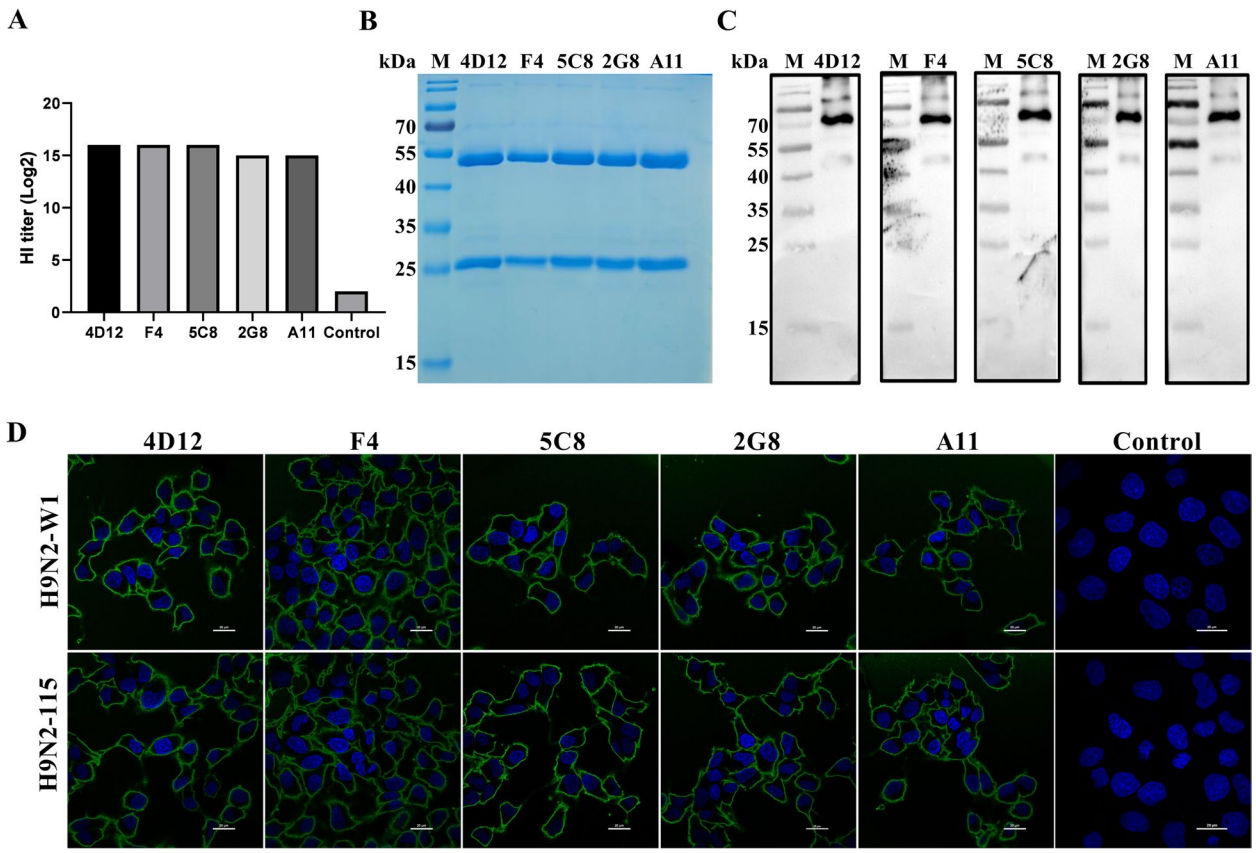

Fig. 3 Reactivities of mAbs to multiple virus strains. **A** HI titer of ascites of mice inoculated with antibody-positive hybridoma cell lines. **B** SDS–PAGE analysis of purified mAbs. **C** Western blot detection of mAb reactivity with H9N2-W1 virus. Inactivated H9N2-W1 viruses were subjected to SDS–PAGE, and western blotting was performed using the mAbs as the primary antibody. **D** Immunofluorescence assay detection of mAb reactivity with H9N2-W1 and H9N2-115 viruses. MDCK cells infected with H9N2-W1 or H9N2-115 were incubated with the mAbs as the primary antibody and FITC-conjugated goat anti-mouse IgG as the secondary antibody. Nuclei were stained with DAPI. Scale bars = 20 μm

Table 2 In vitro neutralization activity of mAbs against multiple virus strains

Neutralization titer (μg/mL)	4D12	F4	5C8	2G8	A11
H9N2-W1	0.078	0.078	0.156	0.156	0.156
H9N2-115	0.078	0.039	0.156	0.078	0.078
H9N2-SH13	0.313	0.313	0.625	0.625	0.625
H1N1-HuB	-	-	-	-	-
H1N1-PR8	-	-	-	-	-

"-" indicates that the antibody does not react with the virus.

Prophylactic efficacy of mAbs against viral infection in vivo

To assess the efficacy of the screened mAbs in vivo, a mouse challenge model was established (Fig. S2A). Five-week-old Balb/c mice were intranasally inoculated with serially diluted H9N2-115 AIV. Only the undiluted virus ($4\times10^{4.5}$ $TCID_{50}$/50 μL) resulted in 100% mortality, and the LD_{50} value of H9N2-115 in mice was determined to be 4×10^{4} $TCID_{50}$ (Fig. S2B-C). Therefore, a challenge dose of $3\times LD_{50}$ was selected for subsequent prophylactic and therapeutic assays. Among the pre-screened mAbs, the F4 mAb showed the highest neutralizing activity (Table 2). Hence, the protective effect of the F4 mAb against lethal infection by H9N2-115 was further evaluated to confirm its prophylactic and therapeutic effects.

For the prophylactic assay, mice were intraperitoneally pre-inoculated with serially diluted F4 mAb and then intranasally challenged with a lethal dose of H9N2-115 AIV at 7 h after mAb inoculation (Fig. 4A). The weight changes and survival rates of the mice were monitored for 14 consecutive days. The results demonstrated a dose-dependent protective effect of F4 mAb against H9N2-115. The protection rates for the 1 μg/g and 3 μg/g dosing groups were 62.5% and 100%, respectively (Fig. 4B-C). This indicated that the F4 mAb effectively prevented lethal infection by H9N2-115 AIV in mice. To assess viral proliferation in the lungs of mice, three mice were randomly selected from each group at 3 days after H9N2-115 challenge. Immunofluorescence showed that control-treated mice exhibited strong fluorescence signals in lung slices, while the fluorescence intensity decreased significantly with pre-inoculated F4 mAb (Fig. 4D). This indicated that the F4 mAb inhibited the proliferation of H9N2-115 AIV in mice lungs. Histopathological observation of the lung tissues from virus-challenged mice showed severe interstitial widening, inflammatory cell infiltration, and alveolar atrophy in the control group. However, as the doses of prophylactic F4 mAb increased, the lung lesions were significantly alleviated. When the administered dose of F4 mAb exceeded 3 μg/g, the lung tissue remained mostly intact (Fig. 4E).

Therapeutic efficacy of mAbs against viral infection in vivo

To determine the therapeutic efficacy of F4 mAb against H9N2-115 AIV infection, mice were intraperitoneally administered serially diluted F4 mAb 7 h after being intranasally challenged with a lethal dose of the virus (Fig. 5A). The weight changes and survival rates were monitored for 14 consecutive days. The results demonstrated a dose-dependent therapeutic effect of F4 mAb against H9N2-115. The protection rate for the 1 μg/g dosing group was 66.6%, and the protection rate reached 100% when the administered F4 mAb dose exceeded 3 μg/g (Fig. 5B-C). Furthermore, the viral load in the mouse lung tissues was determined at 3 and 5 days after dosing with F4 mAb. The results showed a 10- to 15-fold decrease in the viral titers in the 1 μg/g and 3 μg/g dosing groups compared to the control group, and the viral load was barely detectable in the 9 μg/g dosing group at three days of dosing. Moreover, at five days after dosing, the viral loads in the over 3 μg/g dosing groups were undetectable (Fig. 5D). This indicated that the F4 mAb effectively inhibited the proliferation of H9N2-115 in the mouse lung. Histopathological observation of the lungs of mice infected with H9N2-115 in the control group showed moderate to severe bronchiolar necrosis, pulmonary edema, and inflammatory cell infiltration. However, the lung lesions were significantly reduced with the administration of increased doses of the therapeutic F4 mAb. When the administered F4 mAb dose exceeded 3 μg/g, the lung tissue remained basically intact (Fig. 5E).

Discussion

In this study, we successfully screened and identified five mAbs targeting the HA protein of H9N2 AIV. These mAbs, namely 4D12, F4, 5C8, 2G8, and A11, demonstrated potent neutralizing activity in vitro. Further in vivo trials revealed promising preventive and therapeutic effects of the F4 mAb against H9N2-115 infection.

The screened mAbs showed favorable reactivity with H9N2 AIVs in Western blot and immunofluorescence assays. They effectively neutralized H9N2-W1, H9N2-115, and H9N2-SH13 AIVs, with the mAb F4 exhibiting the highest neutralizing potency. Moreover, in vivo prophylactic and therapeutic trials confirmed that intraperitoneal injection of the mAb F4 at a dose of 3 μg/g provided complete protection against lethal H9N2-115 infection, indicating F4 mAb could be used in both prevention and therapy against H9N2 infection. However, none of the screened mAbs demonstrated reactivity with the H1 subtype strains. Thus, the epitopes in HA that the screened neutralizing antibodies specifically bind were supposed to be located in HA1 domain, which was not highly conserved in different subtype strains. Therefore, further validation of the in vitro neutralizing efficacy and

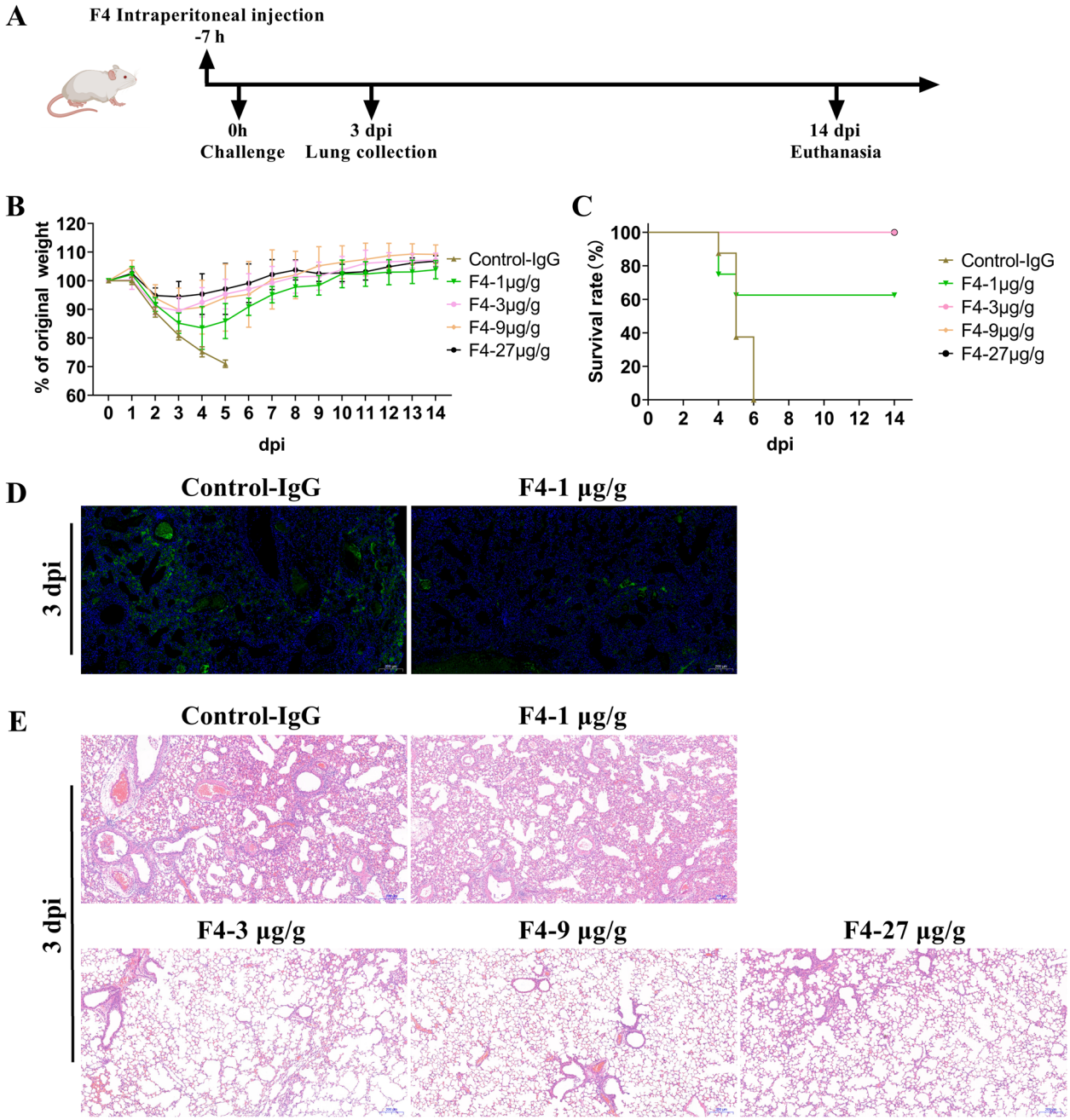

Fig. 4 Prophylactic efficacy of F4 mAb against lethal H9N2-115 challenge. **A** Schematic representation of the prophylactic test. **B** Body weight change of mice following virus challenge. **C** Survival rate of mice after virus challenge. **D** Immunofluorescence staining of lung slices from mice infected with H9N2-115 at 3 dpi. The viral HA antigen was stained green, and the nucleus was stained blue. Scale bars= 200 μm. **E** Histopathological examination of the mouse lungs at 3 dpi. The slices were visualized using hematoxylin and eosin (H&E) staining, scale bars = 200 μm

in vivo protective effects of the F4 mAb against other influenza virus subtypes is necessary. Researchers have made significant efforts to develop a universal neutralizing antibody capable of effectively neutralizing all subtypes of influenza viruses (Corti et al. 2011; Wang et al. 2010). To achieve broad cross-neutralization, several strategies can be employed, including the utilization of highly conserved epitopes of the influenza virus HA protein as immunogens, the combination of multiple antigens (HA, NA, NP and M2e) from the influenza virus, and alternate immunization with antigens derived from different subtypes of influenza viruses (Laursen and

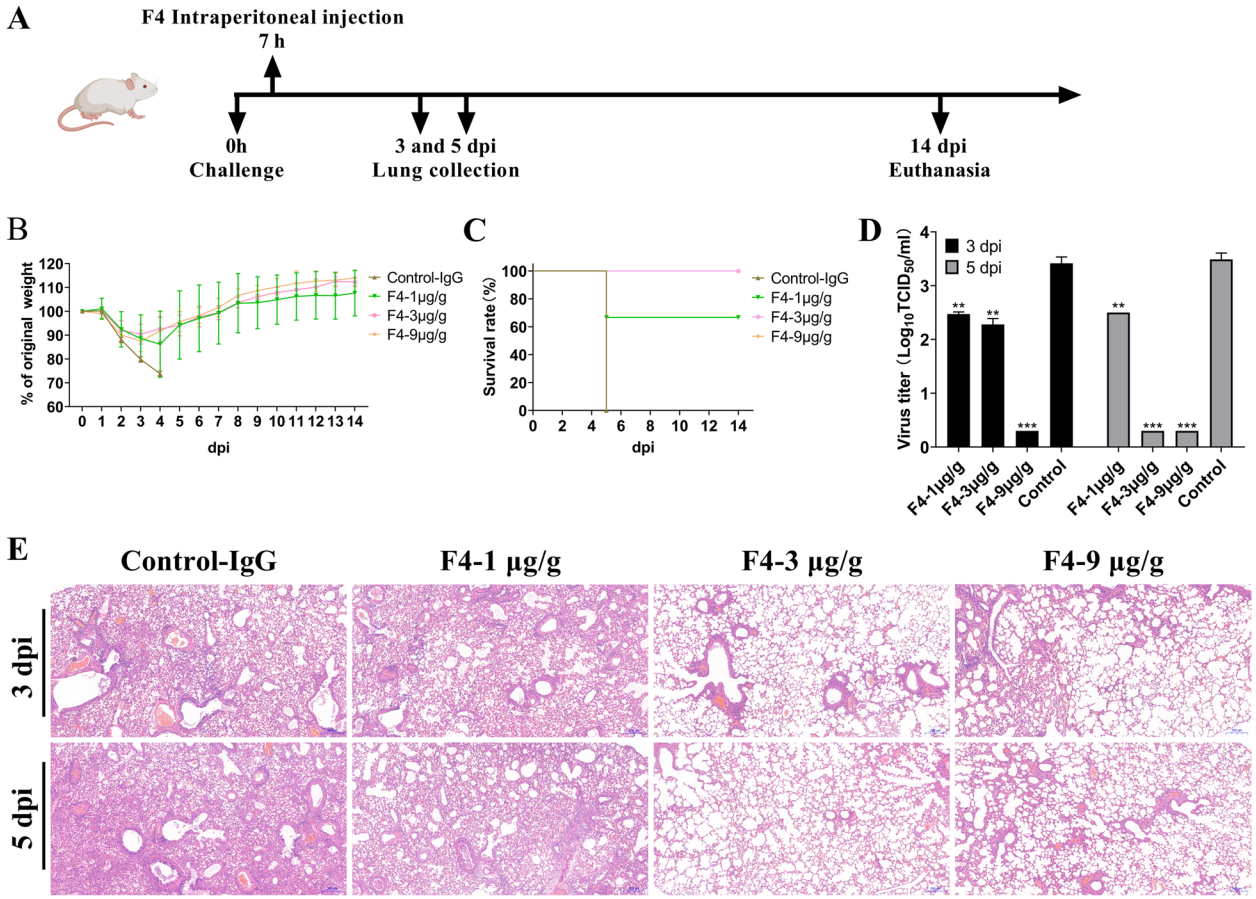

Fig. 5 Therapeutic efficacy of F4 mAb against lethal H9N2-115 infection. **A** Schematic illustration of the therapeutic trial. **B** Body weight change of mice infected with H9N2-115. **C** Survival rate of mice after virus challenge. **D** Virus titers in the lungs of infected mice ($n = 3$) at 3 dpi (left) and 5 dpi (right). Error bars represent means ± SDs. **E** Histopathological examination of lung slices from mice infected with H9N2-115 at 3 dpi and 5 dpi using hematoxylin and eosin (H&E) staining. Scale bars = 200 μm. (**, $p<0.01$; ***, $p<0.001$)

Wilson 2013; Manzoor et al. 2020; Stadlbauer et al. 2019; Sui et al. 2009; Vanderven et al. 2022). Future studies will focus on implementing these strategies to comprehensively screen mAbs with broad neutralizing activities.

Optimizing our screened F4 mAb is necessary due to its suboptimal antiviral effects at low doses in vivo. The efficacy of mAb treatment is highly dependent on the timing of administration. Previous research has demonstrated that administering H1N1 mAb within 6 h after H1N1 influenza virus infection in mice provides complete protection. However, initiating treatment 72 h post-infection reduces the protection rate to 60% (Wang et al. 2022a). In our therapeutic trial, mice were treated with the F4 mAb at 7 h post infection. It would be valuable to further explore the effectiveness of F4 mAb administered at different time points after infection. Therapeutic mAbs often exhibit limited neutralizing activity against specific subtypes of influenza virus, and combining multiple mAbs may enhance therapeutic efficacy. For instance, the combination of CR8020 and CR6261, which target different epitopes, can neutralize a wide range of IAV subtypes (Ekiert et al. 2011). In our animal experiments, we chose the F4 mAb with the highest in vitro neutralization potency as a candidate therapeutic agent. However, the efficacy of the other four mAbs and the potential synergistic effects of their combined administration warrant further investigation.

The humanization of mAbs and optimization of administration routes have greatly accelerated the clinical transformation and application of mAbs (Waldmann 2019). Mouse-derived antibodies can induce immune reactions and generate human anti-mouse antibody responses due to recognition of the constant region by the human immune system (Litzow 2013). Therefore, at the moment, the screened mAbs were put in application only for veterinary use and they should be humanization transformed before being utilized in human. In contrast, humanized antibodies offer high specificity and minimal side effects, making them valuable for treating various diseases, such as cancer, viral infections, and autoimmune

disorders (Mead et al. 2022; Rodriguez-Fernandez et al. 2021; Yang et al. 2022). Humanized antibodies have become the mainstream focus of antibody drug development. Researchers have screened and humanized mAbs against the novel coronavirus, enabling effective prevention and treatment of the disease (Corti et al. 2021b). In our study, the five screened mAbs were murine-derived, which limits their clinical applications. Fully humanizing murine mAbs for emergency treatment of H9N2 influenza infection in humans would be of great significance. Additionally, optimizing antibody administration routes is an effective approach to enhance therapeutic efficacy. During the COVID-19 pandemic, various administration routes have been approved, such as intranasal spray, oral administration, and inhalation (Lu et al. 2022; Qu et al. 2021). In this study, the F4 mAb was administered via intraperitoneal injection. However, optimizing the administration route to oral or intranasal delivery would facilitate its clinical application.

Conclusions

In conclusion, our study identified five mAbs specific to the HA of H9N2 AIV. These mAbs exhibited neutralizing activity against various strains of H9N2 AIVs at the cellular level. Specifically, the F4 mAb exhibited promising preventive and therapeutic effects against lethal H9N2-115 infection in vivo. Our study provides an alternative approach for the prevention and control of H9N2 AIVs.

Methods

Cells and viruses

Madin-Darby canine kidney (MDCK) cells, porcine kidney-15 (PK-15) cells and mouse myeloma cells (SP2/0) were preserved in our laboratory. Cells were maintained in Dulbecco's modified Eagle's medium (Gibco, NY, USA) or RPMI 1640 medium (HyClone, SH30809.01) supplemented with 10% heat-inactivated fetal bovine serum (522 PAN-Biotech, P30-3302) and incubated in a 37°C humidified incubator with 5% CO_2.

Influenza A virus A/duck/Hubei/W1/2004 (H9N2-W1), A/Chicken/Hubei/115/2016 (H9N2-115), A/swine/Hubei/221/2016 (HuB-H1N1) , and A/Puerto Rico/8-SV14/1934 (PR8-H1N1) were preserved in our laboratory. Avian influenza virus A/chicken/Shanghai/SC197/2013 (H9N2-SH13) was kindly gifted by Professor Chengjun Li from Harbin Veterinary Research Institute, CAAS. All viruses were propagated by single passage in embryonic chicken eggs.

Antibodies and reagents

The secondary antibodies used in this study included horseradish peroxidase–conjugated goat anti-mouse IgG (Cat No. BF03001, Beijing Biodragon Inmmunotechnologies, China) and fluorescein isothiocyanate-conjugated goat anti-mouse IgG (Cat No. AS001, Abclonal, China). The reagents used in this study included: 4′,6′-diamidino-2-phenylindole (1:1000) (Cat No. C1002, Beyotime, China); saturated ammonium sulfate solution (Cat No. 9300001001, Leagene Biotechnology, China); HAT medium (Cat No. BF08001, China); octanoic acid (Cat No. C11840809, Macklin, China); and hybridoma feeder (Cat No. MAC0014, Frdbio, China). mAb-isotype Identification Enzyme Kits were purchased from Beijing Biodragon Inmmunotechnologies, China (Cat No. BF16001, China).

Antigen preparation

Avian influenza virus H9N2-W1 was diluted and inoculated into 9- to 11-day-old SPF embryonic chicken eggs. After 72 h, allantoic fluid was collected and centrifuged at 7,000 rpm for 20 min at 4°C to remove cell debris. The viruses were further concentrated by centrifuging at 30,000 rpm for 150 min at 4°C. The viral precipitates were resuspended in PBS and then inactivated by incubating with 1‰ formaldehyde at 37°C and shaking at 180 rpm for 36 h. The inactivated virus was filtered with a 0.22 μm filter for sterilization and stored at -80°C. The inactivation efficiency was assessed by inoculating 9- to 11-day-old SPF embryonic chicken eggs with the inactivated virus, and the hemagglutination titer of the allantoic fluid was determined at 72 h post inoculation.

Cell fusion

SP2/0 myeloma cells were mixed with immunized spleen cells at a 1:10 ratio (1×10^7 myeloma cells per mouse spleen) and centrifuged at 1000 rpm for 10 min. The supernatant was discarded, and the cell precipitate was gently tapped. Next, the cell precipitate was incubated in a 37°C water bath, and 0.8 mL of prewarmed 50% PEG was added with stirring. After stirring for 45 s, the cells were rested for 50 s at 37°C. Then, 40 mL of prewarmed RPMI-1640 medium was slowly added to the cells. The medium was added gradually: 1 mL in the first min, followed by 3 mL over the next 2-5 min. After resting at 37°C for 10 min, the cells were centrifuged at 1000 rpm for 10 min and then resuspended in HAT fusion medium to a final volume of 100 mL. The cells were added dropwise to 96-well plates and cultured at 37°C with 5% CO_2. After 8-10 days of incubation, the medium in the 96-well plate was replaced with 200 μL of HT culture medium. The antibody levels in the culture medium were detected when the cell colony reached 1/4 of the culture well.

Indirect ELISA

Indirect ELISA was used to measure antibody levels in the supernatant of hybridoma cells. Briefly, ELISA plates were coated with inactivated AIVs and incubated at 37°C

for 2 h or at 4°C overnight. After five washes with PBST buffer, the plates were blocked with 3% BSA at 37°C for 2 h or at 4°C overnight. Following three washes with PBST, the hybridoma cell supernatants were added to the plates and incubated at 37°C for 1 h. The plates were then washed five times with PBST and incubated with HRP-conjugated goat anti-mouse IgG at 37°C for 30 min. After extensive PBST washes, TMB substrate was added to each well and incubated for 10 min in the dark. The OD value at 630 nm was determined using a microplate reader after adding the termination solution to each well.

Hemagglutinin inhibition assay

The influenza virus was diluted to a titer of 4 HAU. The supernatants of hybridoma cells were serially twofold diluted, and 35 μL of each diluted supernatant was added to 96-well plates. In each well, except for the PBS control wells, 4 HA units of influenza virus were added. The plates were incubated at room temperature for 25 min, followed by the addition of red blood cells to each well. After incubation at 37°C for 30 min, the HI values were recorded.

Limited dilution assays

A limited dilution assay was used to subclone the antibody-positive hybridoma cells. First, the hybridoma cells were gently blown out from the culture wells and counted using serial dilution. Cells were then diluted in complete culture medium to achieve concentrations of 10, 20 and 50 per milliliter. Each cell suspension was added to 96-well culture plates containing feeder cells, with 100 μL per well. After 10-14 days of subcloning, the culture media were switched to complete media when the cells covered 1/4 to 1/2 of the well. The following day, supernatants were tested for antibody levels. The antibody-positive hybridoma cells were subsequently subcloned again and transferred to a 6-well plate for expansion. Successfully cloned hybridoma cells were cryopreserved for future use.

Chromosome counting and analysis

Upon reaching the logarithmic growth phase, antibody-positive hybridoma cells were treated with colchicine at a final concentration of 0.4 mg/mL. After incubation at 37°C with 5% CO_2 for 3 h, the cells were gently suspended by tapping with a pipette tip. The cell suspension was collected and centrifuged at 1000 rpm for 10 min. The resulting cell pellet was then resuspended in prewarmed KCL (0.075 mol/L) hypotonic solution and incubated in a 37°C water bath for 30 min. Next, 1 mL of freshly prepared fixative solution (methanol: glacial acetic acid = 3:1) was added, mixed, and centrifuged at 1000 rpm for 10 min. The supernatant was discarded, and 1 mL of fresh fixative solution was added, gently mixed, and incubated in a 37°C water bath for 30 min. After another centrifugation step at 1000 rpm for 10 min, the supernatant was removed, and the cell pellet was gently resuspended in 200 μL of fresh fixative solution. Next, 50 μL of the cell suspension was carefully dropped onto a prechilled glass slide, allowing it to air-dry at room temperature. Giemsa staining was then applied to the cells, followed by observation and counting under an oil immersion microscope. Images were captured for documentation.

mAb purification

Eight-week-old Balb/c mice were intraperitoneally injected with 0.5 mL of Freund's incomplete adjuvant per mouse for sensitization. After 7 days, sensitized Balb/c mice were injected with antibody-positive hybridoma cells at a dose of 5×10^5-5×10^6 cells per mouse. Within 7-10 days, ascites of mice with visible abdominal distension were collected. The collected ascites were centrifuged at 1200 rpm for 10 min, and the resulting supernatants were transferred to a clean beaker and gently stirred using a magnetic stirrer. Subsequently. Four times the volume of the ascites of acetate buffer (pH=4.5) was slowly added, followed by the gradual addition of caprylic acid (33 μL/mL). After 30 minutes of stirring at 4°C, the mixture was centrifuged at 12000 rpm for 20 min. The supernatants were then filtered, and the pH was adjusted to 7.4 using ammonia. Then, saturated ammonium sulfate solution was slowly added. The mixture was stirred on a magnetic stirrer for 30 min at 4°C and centrifuged at 12000 rpm for 20 min. The supernatant was discarded, and the resulting pellet was resuspended in PBS for dialysis. For dialysis, the dialysis bag was boiled for 10 min, and the monoclonal antibody suspension was added, sealed, and placed in PBS at 4°C for 24 h. Subsequently, the antibody was stored at -20°C for future use.

Indirect immunofluorescence

For immunofluorescence detection of the reactivity of mAbs with influenza viruses, MDCK cells were incubated with influenza viruses (MOI=50) on ice for 60 min. The cells were subsequently fixed with paraformaldehyde for 15 min. After being washed three times with PBS, the cells were permeabilized with 0.2% Triton X-100 for 15 min. After an intensive wash with PBS, the cells were subsequently blocked with 2% BSA and incubated with mAbs at a concentration of 10 μg/mL at 37°C for 2 h. FITC-conjugated goat anti-mouse antibody was applied as the secondary antibody. The nuclei were stained with DAPI for 10 min at room temperature. The fluorescence signals were observed under a laser confocal microscope.

Viral titration

For viral titration, MDCK cells were washed three times with PBS to remove serum completely. Then, 100 µL of serially diluted virus was added to the wells. After incubation at 37°C for 1 h, the unabsorbed viruses were removed by washing three times with PBS. Then, DMEM supplemented with 0.5 µg/mL N-tosyl-L-phenylalanine chloromethyl ketone (TPCK) trypsin was subsequently added to each well. After incubation for 72 h at 37°C with 5% CO_2, 35 µL of the supernatant from each well was transferred to U-bottomed 96-well microtiter plates, and an equal volume of 1% chicken RBCs was added. The plates were then incubated at 37°C for 25 min. The virus titers were calculated by determining the $\log_{10}TCID_{50}$/mL using the Reed and Muench method.

Neutralization test

The mAbs were serially diluted 2-fold from an initial concentration of 10 µg/mL to 10 gradients, with four replicates per gradient. The diluted mAbs were mixed with an equal volume of 100 $TCID_{50}$/50 µL influenza virus and incubated at 37°C for 2 h. MDCK cells in 96-well plates were washed with PBS and then incubated with the virus-mAb mixture. Positive control wells were supplemented with 100 $TCID_{50}$ virus, while negative control wells received 100 µL diluent. After 72 h of incubation at 37°C with 5% CO_2, 35 µL of supernatant from each well was transferred to U-bottomed 96-well microtiter plates. Then, 1% chicken red blood cells (RBCs) were added, and the plate was incubated at 37°C for 25 min. The half maximal inhibitory concentration (IC_{50}) of the antibody was determined using the hemagglutination inhibition (HI) method.

Prophylactic and therapeutic trials of mAb against influenza virus in vivo

In the prophylactic test, 5-week-old female Balb/c mice were divided into five groups of 11. Groups 1 to 4 were intraperitoneally injected with F4 mAb at different concentrations (1 µg/g, 3 µg/g, 9 µg/g, 27 µg/g), and the control group received an unrelated IgG at a dose of 27 µg/g. After 7 h, mice were intranasally infected with H9N2-115 AIV at a dose of $3\times LD_{50}$. The weight and survival rate of the mice were monitored for 14 days. For the therapeutic trial, 5-week-old female Balb/c mice were divided into four groups of 11. After 7 h of H9N2-115 intranasal infection at a dose of $3\times LD_{50}$, mice in each group were intraperitoneally injected with different doses of F4 mAb (1 µg/g, 3 µg/g, 9 µg/g). Mice in the control group received an unrelated IgG at a dose of 9 µg/g. Weight and survival rate were recorded for 14 consecutive days. On the 3rd and 5th days after H9N2-115 infection, 3 mice from each group were randomly selected and euthanized for viral titration. In the prophylactic test, three mice from each group were randomly selected and euthanized on the 3rd day post-infection for histological examination of lung tissues. In the therapeutic trial, 3 mice from each group were randomly selected and euthanized on the 3rd and 5th days post-infection for histological examination of lung tissues.

Statistical analysis

GraphPad Prism was utilized for all statistical analyses. The data are presented as the means ± standard deviations (SD) from at least three independent experiments. Statistical significance was calculated using Student's two-tailed unpaired t test (ns, $p > 0.05$; *, $p < 0.05$; **, $p < 0.01$; ***, $p < 0.001$).

Supplementary Information

The online version contains supplementary material available at https://doi.org/10.1186/s44149-023-00100-z.

Additional file 1: Figure S1. Phylogenetic tree of haemagglutinin gene of H9N2 subtype influenza viruses. The phylogenetic tree was generated by MEGA using the Maximum Likelihood method. The reliability of the tree was assessed by bootstrap analysis with 1000 replications. Solid black circle indicates segments of reference strains downloaded from GISAID or GenBank, and solid red circle indicates segments sequenced in research.

Additional file 2: Figure S2. Establishment of the H9N2-115 AIV mouse challenge model. (A) Schematic representation of the establishment of the H9N2-115 virus mouse challenge model. (B) Surveillance of mouse body weight following virus challenge. (C) Survival rate of mice after virus challenge.

Acknowledgments

We thank Xiao Xiao for critically proofreading the manuscript.

Authors' contributions

H.Z. and S.S. conceived the project. Y.D., Q.G., G.L., and C.L performed the experiments and organized the data. Y.D., Q.G., S.T., J.Z., Y.C., Y.Z., L.C., and Y.Z. analyzed the data; H.Z., Y.D., S.T., and J.Z. wrote and revised the manuscript. All authors have read and approved the final version of the manuscript.

Funding

This work was supported by the National Key Research and Development Program (2022YFD1801005), the National Natural Science Foundation of China (32025036 and 32060795), the Fundamental Research Funds for the Central Universities (2662023PY005), Hubei Hongshan Laboratory (2022hszd005), the earmarked fund for CARS-41, the Natural Science Foundation of Hubei Province (2021CFA016), and Flexible talent introduction project of Tibet Agricultural and Animal Husbandry College (00000198).

Availability of data and materials

Data will be shared upon request by the readers.

Declarations

Ethics approval and consent to participate

This study was conducted in strict accordance with the recommendations provided in the Guide for the Care and Use of Laboratory Animals of the Ministry of Science and Technology of the People's Republic of China. Animal

experiments were approved by the Hubei Administrative Committee for Laboratory Animals (Approval No. HZAUMO-2023-0145).

Consent for publication
Not applicable.

Competing interests
The author declares that he/she has no competing interests. Author Hongbo Zhou was not involved in the journal's review of, or decisions related to this manuscript.

Received: 26 June 2023 Accepted: 24 September 2023
Published online: 27 November 2023

References

Abed, Y., N. Goyette, and G. Boivin. 2005. Generation and characterization of recombinant influenza A (H1N1) viruses harboring amantadine resistance mutations. *Antimicrobial Agents and Chemotherapy* 49 (2): 556–559. https://doi.org/10.1128/aac.49.2.556-559.2005.

Adlhoch, C., A. Fusaro, J.L. Gonzales, T. Kuiken, S. Marangon, É. Niqueux, C. Staubach, C. Terregino, I. Aznar, I. Muñoz Guajardo, and F. Baldinelli. 2022. Avian influenza overview December 2021 - March 2022. *EFSA Journal. European Food Safety Authority* 20 (4): e07289. https://doi.org/10.2903/j.efsa.2022.7289.

Alexander, D.J. 2007. An overview of the epidemiology of avian influenza. *Vaccine* 25 (30): 5637–5644. https://doi.org/10.1016/j.vaccine.2006.10.051.

Caceres, C.J., B. Seibert, F. Cargnin Faccin, S. Cardenas-Garcia, D.S. Rajao, and D.R. Perez. 2022. Influenza antivirals and animal models. *FEBS Open Bio* 12 (6): 1142–1165. https://doi.org/10.1002/2211-5463.13416.

Carnaccini, S., and D.R. Perez. 2020. H9 influenza viruses: an emerging challenge. *Cold Spring Harbor Perspectives in Medicine* 10 (6): a038588. https://doi.org/10.1101/cshperspect.a038588.

Carter, P.J., and A. Rajpal. 2022. Designing antibodies as therapeutics. *Cell* 185 (15): 2789–2805. https://doi.org/10.1016/j.cell.2022.05.029.

Corti, D., J. Voss, S.J. Gamblin, G. Codoni, A. Macagno, D. Jarrossay, S.G. Vachieri, D. Pinna, A. Minola, F. Vanzetta, et al. 2011. A neutralizing antibody selected from plasma cells that binds to group 1 and group 2 influenza A hemagglutinins. *Science* 333 (6044): 850–856. https://doi.org/10.1126/science.1205669.

Corti, D., N. Passini, A. Lanzavecchia, and M. Zambon. 2016. Rapid generation of a human monoclonal antibody to combat Middle East respiratory syndrome. *Journal of Infection and Public Health* 9 (3): 231–235. https://doi.org/10.1016/j.jiph.2016.04.003.

Corti, D., L.A. Purcell, G. Snell, and D. Veesler. 2021. Tackling COVID-19 with neutralizing monoclonal antibodies. *Cell* 184 (17): 4593–4595. https://doi.org/10.1016/j.cell.2021.07.027.

Corti, D., L.A. Purcell, G. Snell, and D. Veesler. 2021. Tackling COVID-19 with neutralizing monoclonal antibodies. *Cell* 184 (12): 3086–3108. https://doi.org/10.1016/j.cell.2021.05.005.

De Pinho Favaro, M.T., J. Atienza-Garriga, C. Martínez-Torró, E. Parladé, E. Vázquez, J.L. Corchero, N. Ferrer-Miralles, and A. Villaverde. 2022. Recombinant vaccines in 2022: a perspective from the cell factory. *Microbial Cell Factories* 21 (1): 203. https://doi.org/10.1186/s12934-022-01929-8.

Dong, G., C. Peng, J. Luo, C. Wang, L. Han, B. Wu, G. Ji, and H. He. 2015. Adamantane-resistant influenza a viruses in the world (1902–2013): frequency and distribution of M2 gene mutations. *PLoS One* 10 (3): e0119115. https://doi.org/10.1371/journal.pone.0119115.

Dong, J., Y. Zhou, J. Pu, and L. Liu. 2022. Status and challenges for vaccination against avian H9N2 influenza virus in China. *Life (Basel, Switzerland)* 12 (9): 1326. https://doi.org/10.3390/life12091326.

Ekiert, D.C., G. Bhabha, M.A. Elsliger, R.H. Friesen, M. Jongeneelen, M. Throsby, J. Goudsmit, and I.A. Wilson. 2009. Antibody recognition of a highly conserved influenza virus epitope. *Science* 324 (5924): 246–251. https://doi.org/10.1126/science.1171491.

Ekiert, D.C., R.H. Friesen, G. Bhabha, T. Kwaks, M. Jongeneelen, W. Yu, C. Ophorst, F. Cox, H.J. Korse, B. Brandenburg, et al. 2011. A highly conserved neutralizing epitope on group 2 influenza A viruses. *Science* 333 (6044): 843–850. https://doi.org/10.1126/science.1204839.

Gerhard, W., K. Mozdzanowska, and D. Zharikova. 2006. Prospects for universal influenza virus vaccine. *Emerging Infectious Diseases* 12 (4): 569–574. https://doi.org/10.3201/eid1204.051020.

Gu, M., L. Xu, X. Wang, and X. Liu. 2017. Current situation of H9N2 subtype avian influenza in China. *Veterinary Research* 48 (1): 49. https://doi.org/10.1186/s13567-017-0453-2.

Hajam, I.A., J. Kim, and J.H. Lee. 2018. *Salmonella Gallinarum* delivering M2eCD40L in protein and DNA formats acts as a bivalent vaccine against fowl typhoid and H9N2 infection in chickens. *Veterinary Research* 49 (1): 99. https://doi.org/10.1186/s13567-018-0593-z.

Horwood, P.F., S.V. Horm, A. Suttie, S. Thet, Y. Phalla, S. Rith, S. Sorn, D. Holl, S. Tum, S. Ly, E.A. Karlsson, A. Tarantola, and P. Dussart. 2018. Co-circulation of influenza A H5, H7, and H9 viruses and co-infected poultry in live bird markets Cambodia. *Emerging Infectious Diseases* 24 (2): 352–355. https://doi.org/10.3201/eid2402.171360.

Imai, M., M. Yamashita, Y. Sakai-Tagawa, K. Iwatsuki-Horimoto, M. Kiso, J. Murakami, A. Yasuhara, K. Takada, M. Ito, et al. 2020. Influenza A variants with reduced susceptibility to baloxavir isolated from Japanese patients are fit and transmit through respiratory droplets. *Nature Microbiology* 5 (1): 27–33. https://doi.org/10.1038/s41564-019-0609-0.

Kallewaard, N.L., D. Corti, P.J. Collins, U. Neu, J.M. Mcauliffe, E. Benjamin, L. Wachter-Rosati, F.J. Palmer-Hill, A.Q. Yuan, P.A. Walker, M.K. Vorlaender, S. Bianchi, B. Guarino, A. De Marco, F. Vanzetta, G. Agatic, M. Foglierini, D. Pinna, B. Fernandez-Rodriguez, A. Fruehwirth, C. Silacci, R.W. Ogrodowicz, S.R. Martin, F. Sallusto, J.A. Suzich, A. Lanzavecchia, Q. Zhu, S.J. Gamblin, and J.J. Skehel. 2016. Structure and function analysis of an antibody recognizing all influenza a subtypes. *Cell* 166 (3): 596–608. https://doi.org/10.1016/j.cell.2016.05.073.

Kaplon, H., A. Chenoweth, S. Crescioli, and J.M. Reichert. 2022. Antibodies to watch in 2022. *mAbs* 14 (1): 2014296. https://doi.org/10.1080/19420862.2021.2014296.

Kuhn, C., and H.L. Weiner. 2016. Therapeutic anti-CD3 monoclonal antibodies: from bench to bedside. *Immunotherapy* 8 (8): 889–906. https://doi.org/10.2217/imt-2016-0049.

Laursen, N.S., and I.A. Wilson. 2013. Broadly neutralizing antibodies against influenza viruses. *Antiviral Res* 98 (3): 476–483. https://doi.org/10.1016/j.antiviral.2013.03.021.

Li, H., X. Liu, F. Chen, K. Zuo, C. Wu, Y. Yan, W. Chen, W. Lin, and Q. Xie. 2018. Avian influenza virus subtype H9N2 affects intestinal microbiota, barrier structure injury, and inflammatory intestinal disease in the chicken ileum. *Viruses* 10 (5): 270. https://doi.org/10.3390/v10050270.

Li, P., M. Niu, Y. Li, M. Xu, T. Zhao, X. Cao, C. Liang, Y. Wang, Y. Li, and C. Xiao. 2022. Human infection with H3N8 avian influenza virus: a novel H9N2-original reassortment virus. *Journal of Infection* 85 (6): e187–e189. https://doi.org/10.1016/j.jinf.2022.08.033.

Lim, J.J., R. Deng, M.A. Derby, R. Larouche, P. Horn, M. Anderson, M. Maia, S. Carrier, I. Pelletier, T. Burgess, P. Kulkarni, E. Newton, and J.A. Tavel. 2016. Two phase 1, randomized, double-blind, placebo-controlled, single-ascending-dose studies to investigate the safety, tolerability, and pharmacokinetics of an anti-influenza a virus monoclonal antibody, MHAA4549A. *Healthy Volunteers. Antimicrobial agents and chemotherapy* 60 (9): 5437–5444. https://doi.org/10.1128/aac.00607-16.

Litzow, M.R., 2013. Monoclonal antibody-based therapies in the treatment of acute lymphoblastic leukemia. *American Society of Clinical Oncology educational book. American Society of Clinical Oncology. Annual Meeting* 294-299. doi: https://doi.org/10.14694/EdBook_AM.2013.33.294.

Lu, J., Q. Yin, R. Pei, Q. Zhang, Y. Qu, Y. Pan, L. Sun, D. Gao, C. Liang, J. Yang, et al. 2022. Nasal delivery of broadly neutralizing antibodies protects mice from lethal challenge with SARS-CoV-2 delta and omicron variants. *Virologica Sinica* 37 (2): 238–247. https://doi.org/10.1016/j.virs.2022.02.005.

Mahal, A., M. Duan, D.S. Zinad, R.K. Mohapatra, A.J. Obaidullah, X. Wei, M.K. Pradhan, D. Das, V. Kandi, H.S. Zinad, and Q. Zhu. 2021. Recent progress in chemical approaches for the development of novel neuraminidase inhibitors. *RSC Advances* 11 (3): 1804–1840. https://doi.org/10.1039/d0ra07283d.

Manzoor, R., N. Eguchi, R. Yoshida, H. Ozaki, T. Kondoh, K. Okuya, H. Miyamoto, and A. Takada. 2020. A novel mechanism underlying antiviral activity of an influenza Virus M2-specific antibody. *Journal of Virology* 95 (1): e01277-20. https://doi.org/10.1128/jvi.01277-20.

Mead, S., A. Khalili-Shirazi, C. Potter, T. Mok, A. Nihat, H. Hyare, S. Canning, C. Schmidt, T. Campbell, L. Darwent, et al. 2022. Prion protein monoclonal

antibody (PRN100) therapy for Creutzfeldt-Jakob disease: evaluation of a first-in-human treatment programme. *The Lancet Neurology* 21 (4): 342–354. https://doi.org/10.1016/s1474-4422(22)00082-5.
Mortimer, P.P. 2019. Influenza: the centennial of a zoonosis. *Reviews in Medical Virology* 29 (1): e2030. https://doi.org/10.1002/rmv.2030.
Musharrafieh, R., P.I. Lagarias, C. Ma, G.S. Tan, A. Kolocouris, and J. Wang. 2019. The L46P mutant confers a novel allosteric mechanism of resistance toward the influenza A virus M2 S31N proton channel blockers. *Molecular Pharmacology* 96 (2): 148–157. https://doi.org/10.1124/mol.119.116640.
Peacock, T.H.P., J. James, J.E. Sealy, and M. Iqbal. 2019. A global perspective on H9N2 avian influenza virus. *Viruses* 11 (7): 620. https://doi.org/10.3390/v11070620.
Peiris, M., K.Y. Yuen, C.W. Leung, K.H. Chan, P.L. Ip, R.W. Lai, W.K. Orr, and K.F. Shortridge. 1999. Human infection with influenza H9N2. *Lancet* 354 (9182): 916–917. https://doi.org/10.1016/s0140-6736(99)03311-5.
Pusch, E.A., and D.L. Suarez. 2018. The multifaceted zoonotic risk of H9N2 avian influenza. *Veterinary Sciences* 5 (4): 82. https://doi.org/10.3390/vetsci5040082.
Qu, Y., X. Zhang, M. Wang, L. Sun, Y. Jiang, C. Li, W. Wu, Z. Chen, Q. Yin, X. Jiang, Y. Liu, C. Li, J. Li, T. Ying, D. Li, F. Zhan, Y. Wang, W. Guan, S. Wang, and M. Liang. 2021. Antibody cocktail exhibits broad neutralization activity against SARS-CoV-2 and SARS-CoV-2 variants. *Virologica Sinica* 36 (5): 934–947. https://doi.org/10.1007/s12250-021-00409-4.
Rodriguez-Fernandez, R., A. Mejias, and O. Ramilo. 2021. Monoclonal antibodies for prevention of respiratory syncytial virus infection. *The Pediatric Infectious Disease Journal* 40 (5s): S35-s39. https://doi.org/10.1097/inf.0000000000003121.
Shanmuganatham, K., M.M. Feeroz, L. Jones-Engel, G.J. Smith, M. Fourment, D. Walker, L. Mcclenaghan, S.M. Alam, M.K. Hasan, P. Seiler, et al. 2013. Antigenic and molecular characterization of avian influenza A (H9N2) viruses, Bangladesh. *Emerging Infectious Diseases* 19 (9): 1393–1402. https://doi.org/10.3201/eid1909.130336.
Stadlbauer, D., X. Zhu, M. Mcmahon, J.S. Turner, T.J. Wohlbold, A.J. Schmitz, S. Strohmeier, W. Yu, R. Nachbagauer, P.A. Mudd, I.A. Wilson, A.H. Ellebedy, and F. Krammer. 2019. Broadly protective human antibodies that target the active site of influenza virus neuraminidase. *Science* 366 (6464): 499–504. https://doi.org/10.1126/science.aay0678.
Subbarao, K., and T. Joseph. 2007. Scientific barriers to developing vaccines against avian influenza viruses. *Nature Reviews Immunology* 7 (4): 267–278. https://doi.org/10.1038/nri2054.
Sui, J., W.C. Hwang, S. Perez, G. Wei, D. Aird, L.M. Chen, E. Santelli, B. Stec, G. Cadwell, M. Ali, et al. 2009. Structural and functional bases for broad-spectrum neutralization of avian and human influenza A viruses. *Nature Structural & Molecular Biology* 16 (3): 265–273. https://doi.org/10.1038/nsmb.1566.
Takashita, E., C. Kawakami, H. Morita, R. Ogawa, S. Fujisaki, M. Shirakura, H. Miura, K. Nakamura, N. Kishida, T. Kuwahara, K. Mitamura, T. Abe, M. Ichikawa, M. Yamazaki, S. Watanabe, and T. Odagiri. 2019. Detection of influenza A (H3N2) viruses exhibiting reduced susceptibility to the novel cap-dependent endonuclease inhibitor baloxavir in Japan, December 2018. *Euro Surveillance : Bulletin Européen Sur Les Maladies Transmissibles = European Communicable Disease Bulletin* 24 (3): 1800698. https://doi.org/10.2807/1560-7917.Es.2019.24.3.1800698.
Vanderven, H.A., R. Esterbauer, S. Jegaskanda, H.X. Tan, A.K. Wheatley, and S.J. Kent. 2022. Poor protective potential of influenza nucleoprotein antibodies despite wide prevalence. *Immunology & Cell Biology* 100 (1): 49–60. https://doi.org/10.1111/imcb.12508.
Waldmann, H. 2019. Human monoclonal antibodies: the benefits of humanization. *Methods in Molecular Biology* 1904: 1–10. https://doi.org/10.1007/978-1-4939-8958-4_1.
Wang, T.T., G.S. Tan, R. Hai, N. Pica, E. Petersen, T.M. Moran, and P. Palese. 2010. Broadly protective monoclonal antibodies against H3 influenza viruses following sequential immunization with different hemagglutinins. *PLOS Pathogens* 6 (2): e1000796. https://doi.org/10.1371/journal.ppat.1000796.
Wang, L., F. Yang, Y. Xiao, B. Chen, F. Liu, L. Cheng, H. Yao, N. Wu, and H. Wu. 2022. Generation, characterization, and protective ability of mouse monoclonal antibodies against the HA of A (H1N1) influenza virus. *Journal of Medical Virology* 94 (6): 2558–2567. https://doi.org/10.1002/jmv.27584.
Wang, W.C., Sayedahmed, E.E., Sambhara, S., Mittal, S.K., 2022b. Progress towards the Development of a Universal Influenza Vaccine. *Viruses* 14 (8). doi: https://doi.org/10.3390/v14081684.
Wollacott, A.M., M.F. Boni, K.J. Szretter, S.E. Sloan, M. Yousofshahi, K. Viswanathan, S. Bedard, C.A. Hay, P.F. Smith, Z. Shriver, and J.M. Trevejo. 2016. Safety and upper respiratory pharmacokinetics of the hemagglutinin stalk-binding antibody VIS410 support treatment and prophylaxis based on population modeling of seasonal influenza a outbreaks. *EBioMedicine* 5: 147–155. https://doi.org/10.1016/j.ebiom.2016.02.021.
Xu, K.M., K.S. Li, G.J. Smith, J.W. Li, H. Tai, J.X. Zhang, R.G. Webster, J.S. Peiris, H. Chen, and Y. Guan. 2007. Evolution and molecular epidemiology of H9N2 influenza A viruses from quail in southern China, 2000 to 2005. *Journal of Virology* 81 (6): 2635–2645. https://doi.org/10.1128/jvi.02316-06.
Yang, F., S. Yan, L. Zhu, F.X.C. Wang, F. Liu, L. Cheng, H. Yao, N. Wu, R. Lu, and H. Wu. 2022. Evaluation of panel of neutralising murine monoclonal antibodies and a humanised bispecific antibody against influenza A (H1N1) pdm09 virus infection in a mouse model. *Antiviral Research* 208: 105462. https://doi.org/10.1016/j.antiviral.2022.105462.

Publisher's Note